

A Novel Miniaturized UWB Bandpass Filter Basing on E-Shaped Defected Microstrip Structure

Lichang Huang¹, Minquan Li^{1, *}, Pingjuan Zhang², and Kaiyue Duan¹, Yawen Song¹

Abstract—This paper proposes a novel miniaturized UWB bandpass filter by cascading two miniaturized low-pass and high-pass modules. On account of the slow wave and stopband characteristic of defected microstrip structure (DMS), an E-shaped DMS with low-pass characteristic is presented, and an RLC equivalent circuit is utilized to analyze it. By three-dimensional electromagnetic modeling, the S parameters can be obtained to extract the initial parameter values of the RLC equivalent circuit and verify the validity of equivalent circuit in Advanced Design System. The high-pass module uses a lump element to reduce the circuit dimension. The high frequency selectivity can be achieved by loading L-shaped stubs, which produces one transmission zero at the upper band of passband and has a good rectangle coefficient of 1.2 (25 dB-bandwidth/3 dB-bandwidth). To verify the idea, a compact UWB bandpass filter is simulated and fabricated. The result shows that the passband range is 3.1–10.6 GHz with 1 dB loss, and the measurement has a good agreement with the simulation. Besides, a notched wave working in X wave band can also be generated. Compared with the previous works, this UWB bandpass filter has the advantages of miniature and high selectivity.

1. INTRODUCTION

Since the Federal Communications Commission announced the ultra-wideband (UWB) frequency (3.1–10.6 GHz), the study of UWB technology has become more and more popular. Filter is an important component of Wireless Communication Systems; therefore, the research on UWB bandpass filter (BPF) also attracts attention from many researchers. Recently, there are several main UWB technologies as follows: Firstly, two transmission zeroes at the lower and upper bands are generated by loading short-circuit or open-circuit resonators, and coupling multimode resonator is also a common technology, which puts multiple resonant modes together to form a UWB [1–9]. A quintuple-mode UWB BPF is presented, which has a great frequency selectivity by loading open and short stubs at asymmetric parallel-coupled lines in [8], but it has larger size of $0.645\lambda_g \times 0.318\lambda_g$ at 6.85 GHz. In [9], a UWB filter with high selectivity and ultra-wide stopband is proposed by loading fan-shaped stubs, and the size is $0.60\lambda_g \times 0.54\lambda_g$. Secondly, a compact differential UWB bandpass filter is presented in [10], which utilizes difference-mode and common-mode to form the passband and stopband, respectively. Thirdly, multilayer liquid crystal polymer technology is also used to design a UWB bandpass filter [11, 12]. Then, UWB bandpass filter usually uses a defected ground structure (DGS) that a specific defected structure is etched in the ground of a microstrip structure with low-pass or high-pass characteristic, which produces an attenuation pole at the lower or upper bands to create a UWB [13, 14]. In [13], a highpass filter is given and suppresses the upper-band harmonics by etching a SIR-shaped DGS, and the dimension of the proposed filter is $22 \times 10 \text{ mm}^2$. Finally, some algorithms are also used to calculate the electrical parameter of the circuit, and then the UWB bandpass filter can be designed [15, 16]. Above

Received 26 June 2020, Accepted 12 August 2020, Scheduled 1 September 2020

* Corresponding author: Minquan Li (AHU411MHz@hotmail.com).

¹ Key Lab of Ministry of Education of Intelligent Computing & Signal Processing, Anhui University, Hefei 230601, China. ² Anhui Science and Technology University, Bengpu 233100, China.

all, these filters have a good UWB characteristic, but their sizes are still large. This paper presents a novel miniaturized UWB bandpass filter with a little smaller size.

Because the defected ground structure easily causes power leakage, which affects the other components of integrated circuit system, the defected microstrip structure (DMS) appears. Since the DMS is proposed, it gets extensive application especially in the filter designing. The DMS is used to design stopband filter [17–21], bandpass filter [22], suppress spurious response [23, 24], notch band [25, 26], UWB bandpass filter [27]. Because there is little study on a UWB BPF based on DMS only and the dimension of a UWB bandpass filter is a bit larger than the DMS UWB bandpass filter, a miniaturized UWB bandpass filter based on an E-shaped DMS is proposed in this paper. In order to remove undesired signal, a notch band operating on X wave band can be achieved, and the location of the notch band can be controlled by adjusting the length of the stub.

2. DESIGN AND ANALYSIS

2.1. E-Shaped Defected Microstrip Structure

The new E-shaped DMS is presented in Figure 1(a), which etches an E-shaped slot on the microstrip line. The E-shaped slot changes the current path and increases the length of current path. In addition, because of the additional inductive effect of an E-shaped slot, the E-shaped DMS has the characteristic of stopband and slow wave. In Figure 1(b), an RLC equivalent circuit is used to analyze the E-shaped DMS, and the circuit parameters refer to [24]. The ABCD matrix is utilized to derive it and the matrix equation as follows:

$$\begin{bmatrix} A & B \\ C & D \end{bmatrix} = \begin{bmatrix} 1 & Z_G \\ 0 & 1 \end{bmatrix} \begin{bmatrix} 1 & 1/Y \\ 0 & 1 \end{bmatrix} \begin{bmatrix} 1 & 0 \\ 1/Z_L & 1 \end{bmatrix} = \begin{bmatrix} 1 + (1/Y + Z_G)/Z_L & 1/Y + Z_G \\ 1/Z_L & 1 \end{bmatrix} \quad (1)$$

where $Z_G = Z_L = Z_0$, $Y = 1/R + j(\omega C - 1/(\omega L))$, Z_0 is the port impedance.

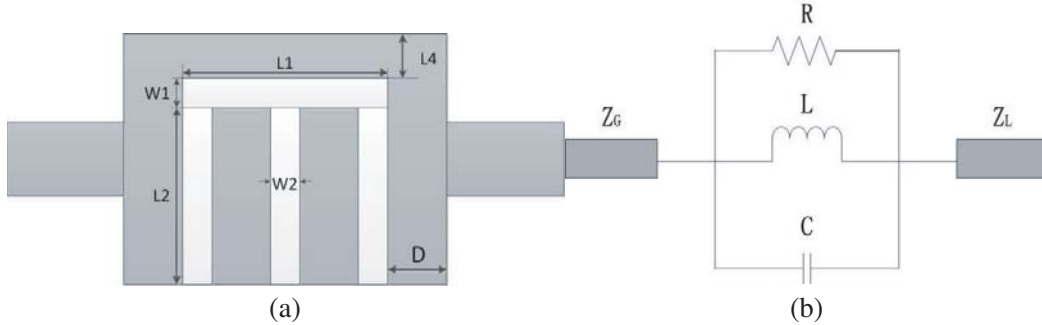


Figure 1. (a) E-shaped DMS, (b) The equivalent RLC circuit of E-shaped DMS.

Because the DMS has a band-stop response, the transfer function can be described as:

$$S_{21}(\omega) = 2Z_0 / (2Z_0 + 1/Y) \quad (2)$$

When the RLC circuit is resonant, the electric field energy is equal to magnetic energy, $Z = 1/Y = R$; therefore, the R value can be obtained

$$R = 2Z_0 (1/|S_{21}(\omega)| - 1) / f = f_r \quad (3)$$

According to $Q = \omega_r CR$ and $BW = f_r/Q$, the C value can be realized. Meanwhile, the L value can also be generated from Equation (5).

$$C = 1/(2\pi R * BW) \quad (4)$$

$$f_r = 1/(2\pi\sqrt{LC}) \quad (5)$$

$$L = \frac{1}{(2\pi f_r)^2 C} \quad (6)$$

where f_r is the resonant frequency, and BW is the -25 dB bandwidth of $S_{21}/f = f_r$, but the sideband selectivity of band-stop response is not great. According to the above equation, we can know that the quality factor is proportional to the C value. So, a correction faction δ is introduced to freely adjust the sideband selectivity, as Equation (7):

$$C = \frac{1}{2\pi R * BW} (1 + \delta) \tag{7}$$

In this study, the S parameters can be extracted by three-dimensional electromagnetic modeling. The simulation result shows that $S_{21}/f = f_r$ is -32 dB, and the -25 dB bandwidth is 0.4 GHz. In Figure 2(a), it is shown that the sideband becomes sharp with the increase of δ , but the sideband cannot be too sharp, which affects the next out-of-band rejection. Therefore, according to Equations (3), (4), (6), (7), the initial parameter value can be calculated as: $R = 3881 \Omega$, $\delta = 1.5$, $C = 0.2500$ pF, $L = 1.0132$ nH. In order to verify the validity of equivalent circuit, the circuit is simulated by Advanced Design System. And the circuit response and full-wave simulation results are depicted in Figure 2(b), which demonstrates that the circuit response has a good agreement with full-wave simulation.

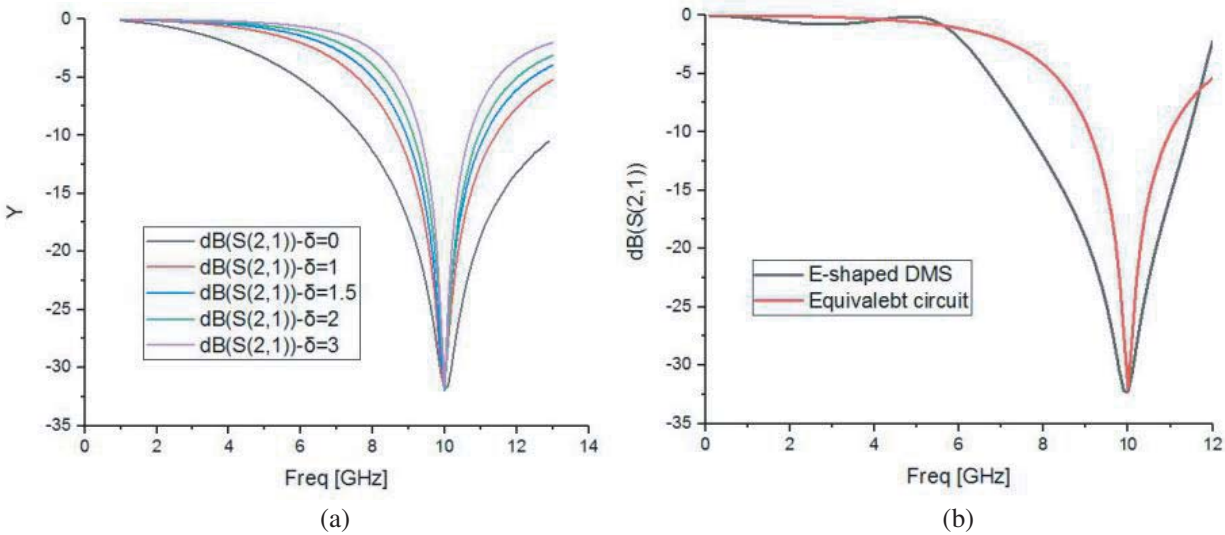


Figure 2. (a) Sweeping the parameter δ . (b) The circuit response and full-wave simulation results.

To research the relation between E-shaped DMS parameters and electrical property, some parameters are studied and analyzed. From Figure 3(a), with the increase of $L1$, the additional inductance gets larger, hence, the resonant frequency moves to lower frequency. Figure 3(b) displays that the additional capacitance becomes smaller with the growth of $W2$; therefore, the resonant frequency moves to upper frequency. In Figure 3(c), the additional effect shows a inductance characteristic with the augment of $W1$. So, the resonant characteristic also moves to lower frequency.

According to aforementioned analysis, we can adjust several main parameters to control the resonant characteristic. Finally, an E-shaped DMS with low-pass characteristic is presented, which serves as an important module of the UWB bandpass filter. The simulation result is demonstrated in Figure 4.

2.2. Semi-Lumped High-Pass Module

In this paper, a third order Chebyshev high-pass filter is chosen. By looking up information, normalized low-pass element values can be confirmed: $g1 = g3 = 1.0315$, $g2 = 1.1474$. The high-pass filter can be achieved by transforming a normalized low-pass prototype, and the lump prototype is presented in Figure 5(a). The shunt inductance can be transformed to a short-circuit microstrip line, as follows:

$$l = \frac{11.81L}{Z0\sqrt{\epsilon_r}} \tag{8}$$

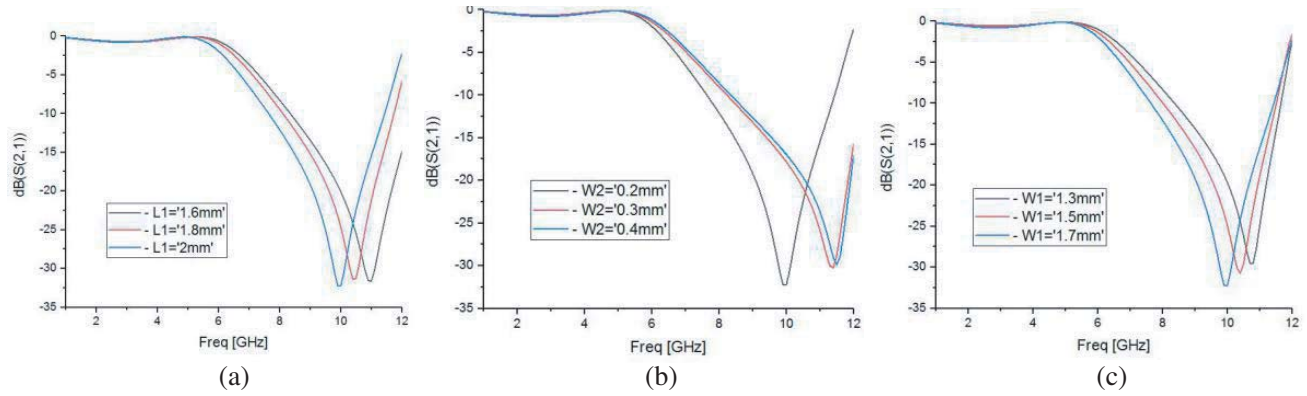


Figure 3. The resonant characteristic of E-shaped DMS.

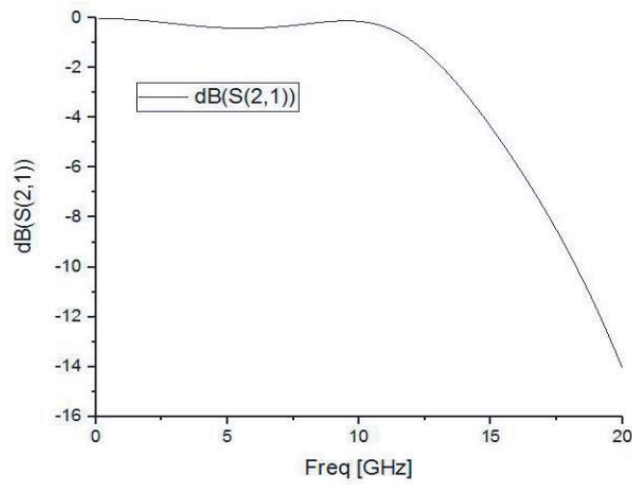


Figure 4. Frequency response of E-shaped DMS.

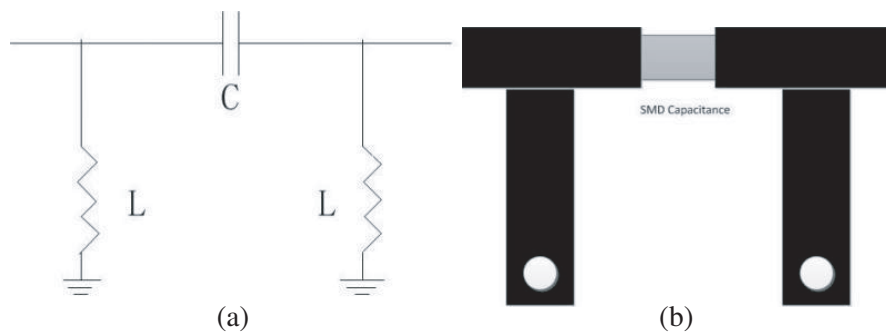


Figure 5. (a) The topological structure of high-pass module. (b) Semi-lumped high-pass module.

where l is the length of microstrip line (unit: inch), and L is inductance value (unit: nH).

In design, a Murata GRM18 SMD capacitor of 0.5 pF is used to miniaturize the size of UWB bandpass filter, and the semi-lumped structure is given in Figure 5(b).

Then, the semi-lumped model can be simulated and optimized by ADS software, and the simulation result is shown in Figure 6.

The miniaturized UWB bandpass filter can be realized by cascading the E-shaped DMS with a semi-lumped module.

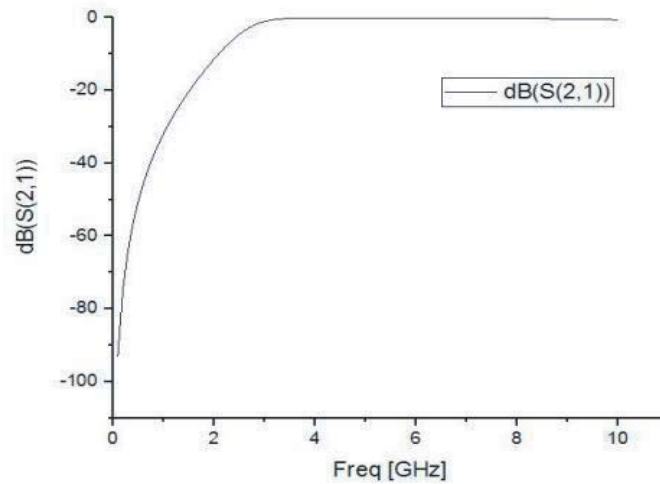


Figure 6. Frequency response of semi-lumped high-pass module.

3. SIMULATION RESULTS AND MEASUREMENT

To verify this approach, the miniaturized UWB bandpass filter is simulated and implemented on a 0.508 mm-thick Rogers Ro5880 substrate which has a loss tangent of 0.0009 and relative dielectric constant ϵ_r of 2.2.

3.1. Simulation Results

The microstrip structure of the UWB bandpass filter is presented in Figure 7, and the physical parameters are exhibited in Table 1. Compared with previous works, the UWB bandpass filter has a smaller size with $12.6 \text{ mm} \times 8.3 \text{ mm}$ ($0.4\lambda_g \times 0.26\lambda_g$) and great return loss above 22 dB. There is a systematic comparison in Table 2.

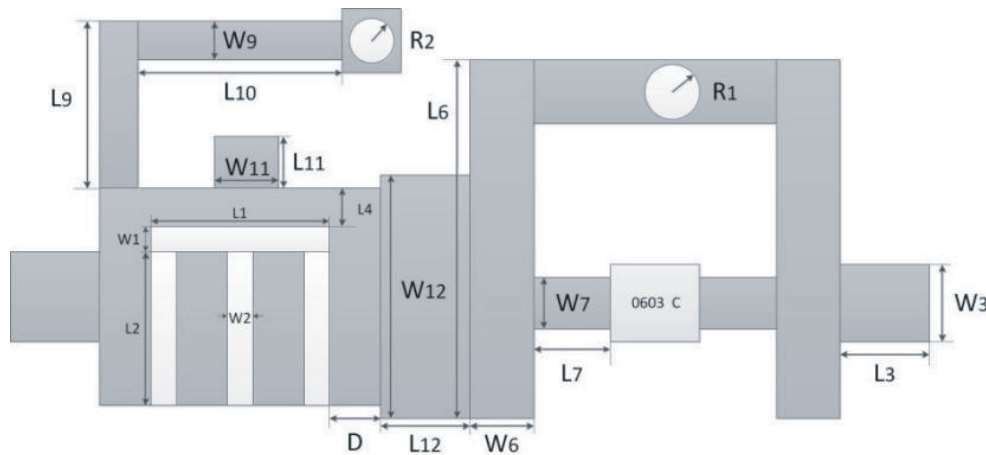


Figure 7. The general structure of miniaturized UWB bandpass filter.

The final simulation result is given in Figure 8. It is shown that the passband range is 3.1–10.6 GHz, and the frequency selectivity is also great.

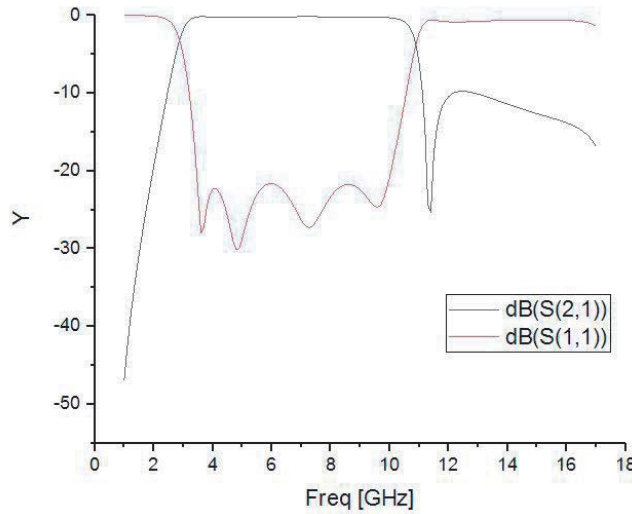
Besides, with the total dimension being almost the same, a notched band is generated by adding an L-shaped resonator. By controlling the length of the L-shaped resonator, the notched wave can operate on X band, and the parameter-sweep result is demonstrated in Figure 9.

Table 1. Physical parameters of miniaturized UWB bandpass filter (unit: mm).

| | | | | | | | | | | |
|------|------|------|------|-------|-------|-------|-------|-------|------|------|
| $L1$ | $W1$ | $L2$ | $W2$ | $L3$ | $W3$ | $L4$ | D | $L6$ | $W7$ | $R1$ |
| 0.8 | 1.3 | 1.6 | 0.2 | 0.8 | 2.1 | 0.2 | 1.1 | 7.2 | 0.6 | 0.4 |
| $L7$ | $W6$ | $L9$ | $W9$ | $L10$ | $L11$ | $W11$ | $L12$ | $W12$ | $R2$ | |
| 1 | 1.2 | 5.2 | 0.3 | 4 | 1.6 | 1.6 | 2 | 3.2 | 0.15 | |

Table 2. Comparison of various UWB bandpass filter.

| Reference | Return Loss (dB) | Size ($\lambda_g \times \lambda_g$), at 6.85 GHz | Upper Stopband (GHz) | Roll off rate/GHz Lower, Upper |
|-----------|------------------|----------------------------------------------------|----------------------|-----------------------------------|
| [6] | ≥ 15 | 0.89×0.21 | 14 | 83.33 dB, 100 dB |
| [8] | ≥ 12 | 0.645×0.318 | 17 | 50 dB, 16.67 dB |
| [9] | ≥ 17 | 0.60×0.54 | 15 | 55.56 dB, 22.73 dB |
| [10] | ≥ 16 | 0.93×1.06 | 14 | 19.23 dB, 13.89 dB |
| [13] | ≥ 15 | 0.63×0.31 | 25 | 5.66 dB, 15 dB |
| [15] | ≥ 17 | 0.92×0.47 | 14 | 10 dB, 31.25 dB |
| [16] | ≥ 15 | 0.59×0.63 | 20 | 10 dB, 7.5 dB |
| [26] | ≥ 16 | 0.42×0.84 | 13 | 35.71 dB, 25 dB |
| [27] | ≥ 12 | 1.4×0.07 | 16 | 13.79 dB, 15.38 dB |
| This Work | ≥ 22 | 0.4×0.26 | 18 | 16.66 dB, 23.8 dB |

**Figure 8.** Frequency response of miniaturized UWB bandpass filter.

3.2. Measurement and Analysis

To validate this idea, a miniaturized UWB BPF has been fabricated and tested shown in Figure 10(a) and Figures 10(b), (c), respectively. In Figure 10(c), we can know that group delay is better than 0.6 ns in the whole passband. In Figure 10(b), it is shown that the return loss is better than 12 dB, and the insertion loss is better than 2.6 dB. Due to mismatching tolerance and parasitic effect of soldering, the return loss becomes worse than simulation result. Moreover, a chip capacitor that has good characteristic at high

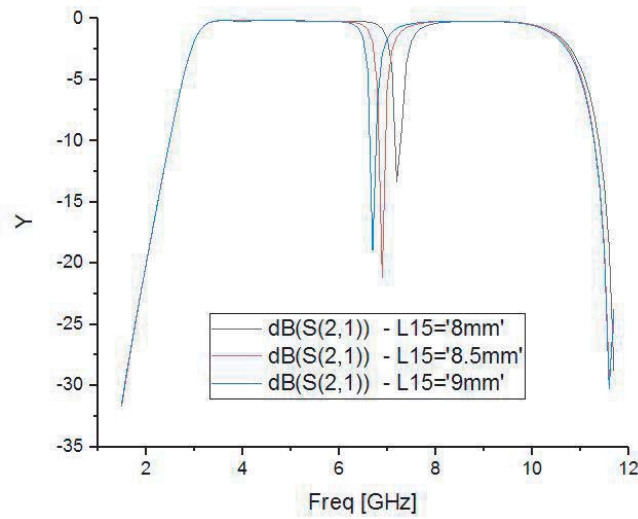


Figure 9. Frequency response of miniaturized UWB bandpass filter with a notch band.

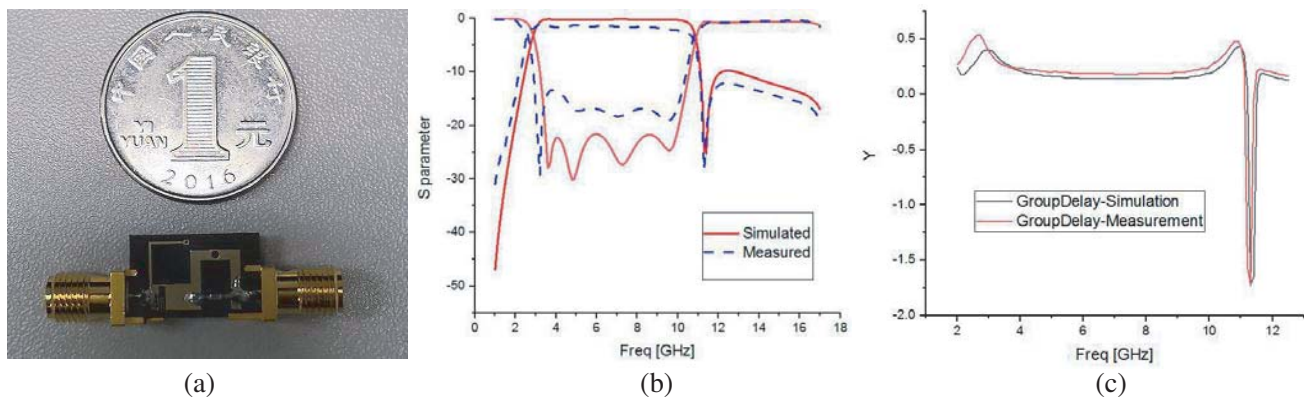


Figure 10. (a) Fabricated prototype. (b) Measurement result. (c) Group delay.

frequency is utilized to reduce the circuit size, but it has a parasitic resistance and welding parasitic capacitance. Therefore, the insertion loss gets a little larger. As the capacitance value gets larger, the lower sideband of passband moves to lower frequency, and the matching degree becomes worse. Although the measurement results are a little different from simulation, it is acceptable. Besides, we can find that the stopband attenuation is better than simulation, because the parasitic resistance is larger at high frequency.

4. CONCLUSION

In this letter, a novel miniaturized UWB bandpass filter based on an E-shaped DMS is proposed. Firstly, the E-shaped DMS is designed and analyzed by using an equivalent circuit. Then, a semi-lumped high-pass module is designed in order to further decrease the dimension. Finally, a miniaturized UWB bandpass filter is designed and fabricated by cascading the E-shaped DMS and semi-lumped high-pass module. The result shows that this approach is right, and it has smaller size and great return loss compared with previous works.

ACKNOWLEDGMENT

This work is supported by the Key Natural Science Research Project of Anhui Higher Education Institutions: Research on Environmental RF Energy Harvesting System KJ2019A0804, and the National Nature Science Foundation of China 51477001.

REFERENCES

1. Wei, F., et al., "Compact UWB bandpass filter with triple-notched bands using triple-mode stepped impedance resonator," *IEEE Microwave and Wireless Components Letters*, Vol. 22, No. 10, 512–514, 2012.
2. Kamma, A., et al., "Multi mode resonators based triple band notch UWB filter," *IEEE Microwave and Wireless Components Letters*, Vol. 27, No. 2, 120–122, 2017.
3. Kumar, S., R. D. Gupta, and M. S. Parihar, "Multiple band notched filter using C-shaped and E-shaped resonator for UWB applications," *IEEE Microwave and Wireless Components Letters*, Vol. 26, No. 5, 340–342, 2016.
4. Zhang, X. Y., Y. W. Zhang, and Q. Xue, "Compact band-notched UWB filter using parallel resonators with a dielectric overlay," *IEEE Microwave and Wireless Components Letters*, Vol. 23, No. 5, 252–254, 2013.
5. Xu, J., et al., "Compact UWB bandpass filter with a notched band using radial stub loaded resonator," *IEEE Microwave and Wireless Components Letters*, Vol. 22, No. 7, 351–353, 2012.
6. Shang, Z., et al., "Design of a superconducting Ultra-Wideband (UWB) bandpass filter with sharp rejection skirts and miniaturized size," *IEEE Microwave and Wireless Components Letters*, Vol. 23, No. 2, 72–74, 2013.
7. Li, X. and X. Ji, "Novel compact UWB bandpass filters design with cross-coupling between $\lambda/4$ short-circuited stubs," *IEEE Microwave and Wireless Components Letters*, Vol. 24, No. 1, 23–25, 2014.
8. Xia, X., X. Cheng, F. Chen, and X. Deng, "Compact UWB bandpass filter with sharp roll-off using APCL structure," *Electronics Letters*, Vol. 54, No. 13, 837–839, June 28, 2018.
9. Zhou, C., P. Guo, K. Zhou, and W. Wu, "Design of a compact UWB filter with high selectivity and superwide stopband," *IEEE Microwave and Wireless Components Letters*, Vol. 27, No. 7, 636–638, July 2017.
10. Aliqab, K. and J. Hong, "Wideband differential-mode bandpass filters with stopband and common-mode suppression," *IEEE Microwave and Wireless Components Letters*, Vol. 30, No. 3, 233–236, March 2020.
11. Hao, Z. C. and J. S. Hong, "UWB bandpass filter using cascaded miniature high-pass and low-pass filters with multilayer liquid crystal polymer technology," *IEEE Transactions on Microwave Theory and Techniques*, Vol. 58, No. 4, 941–948, 2010.
12. Hao, Z.-C. and J.-S. Hong, "Quasi-elliptic UWB bandpass filter using multilayer liquid crystal polymer technology," *IEEE Microwave and Wireless Components Letters*, Vol. 20, No. 4, 202–204, 2010.
13. Sarkar, P., et al., "Compact UWB bandpass filter with dual notch bands using open circuited stubs," *IEEE Microwave and Wireless Components Letters*, Vol. 22, No. 9, 453–455, 2012.
14. Lin, W. J., et al., "Investigation in open circuited metal lines embedded in defected ground structure and its applications to UWB filters," *IEEE Microwave and Wireless Components Letters*, Vol. 20, No. 3, 148–150, 2010.
15. Zhao, J., et al., "Compact microstrip UWB bandpass filter with dual notched bands using E-shaped resonator," *IEEE Microwave and Wireless Components Letters*, Vol. 23, No. 12, 638–640, 2013.
16. Yun, Y. C., et al., "Optimal design of a compact filter for UWB applications using an improved particle swarm optimization," *IEEE Transactions on Magnetics*, Vol. 52, No. 3, 1–4, 2016.

17. Xiao, J. K. and Y. F. Zhu, "Multi-band bandstop filter using inner T-shaped Defected Microstrip Structure (DMS)," *AEU International Journal of Electronics & Communications*, Vol. 68, No. 2, 90–96, 2014.
18. Kazerooni, M., M. A. Salari, A. Cheldavi, and M. Kamarei, "Analysis and modelling of novel band stop and band pass millimeter wave filters using defected microstrip structure (DMS)," *2009 First Conference on Millimeter-Wave and Terahertz Technologies (MMWaTT)*, 1–4, Tehran, 2009, doi: 10.1109/MMWATT.2009.5450468.
19. La, D., Y. Lu, and S. Sun, "Novel bandstop filter using dual-U shape defected microstrip structure," *2010 International Symposium on Signals, Systems and Electronics*, 1–3, Nanjing, 2010.
20. La, D., et al., "A novel compact bandstop filter using defected microstrip structure," *Microwave & Optical Technology Letters*, Vol. 53, No. 2, 433–435, 2011.
21. Zheng, X., "Dual UWB bandstop filter based on M-shaped defected microstrip structure," *2017 Progress In Electromagnetics Research Symposium — Spring (PIERS)*, St. Petersburg, Russia, May 22–25, 2017.
22. Xiao, J. K., et al., "Controllable miniature tri-band bandpass filter using defected microstrip structure," *Electronics Letters*, Vol. 50, No. 21, 1534–1536, 2014.
23. Moyra, T., "Performance improvement of parallel coupled band-pass filter using defected microstrip structure," *IJCA Proceedings on International Conference on Communication, Circuits and Systems 2012*, 2013.
24. Fallahzadeh, S., A. Akbarzadeh, and M. Tayarani, "Spurious response suppression in microstrip bandpass filters using defected microstrip structures," *Electromagnetics*, Vol. 32, No. 7, 389–400, 2012.
25. Wang, Y., T. Jiang, and Y. Li, "A miniaturized ultra-wideband band-pass filter with narrowband anti-interference characteristics," *2015 Asia-Pacific Microwave Conference (APMC)*, IEEE, 2015.
26. Firmansyah, T., G. Wibisono, and E. T. Rahardjo, "Compact UWB bandpass filter based on crossed dumbbell-stub with notch band using defected microstrip structure," *2019 16th International Conference on Quality in Research (QIR): International Symposium on Electrical and Computer Engineering*, 1–5, Padang, Indonesia, 2019.
27. Fallahzadeh, S. and M. Tayarani, "A new microstrip UWB bandpass filter using defected microstrip structures," *Journal of Electromagnetic Waves and Applications*, Vol. 24, No. 7, 893–902, 2010.